

FREEZE-DRIED BINARY AND TERNARY SOLID DISPERSIONS OF CANNABIDIOL: FORMULATION, CHARACTERIZATION, AND SOLUBILITY ENHANCEMENT

THANAPORN JUNTANON¹, NETI WARANUCH^{1,3}, KORNBANOK INGGANINAN^{2,3}, TASANA PITAKSUTTEEPONG^{1,3,4*}

¹Department of Pharmaceutical Technology, Faculty of Pharmaceutical Sciences, Naresuan University, Phitsanulok-65000, Thailand. ²Department of Pharmaceutical Chemistry and Pharmacognosy, Faculty of Pharmaceutical Sciences, Naresuan University, Phitsanulok-65000, Thailand. ³Center of Excellence for Innovation in Chemistry, Faculty of Pharmaceutical Sciences, Naresuan University, Phitsanulok-65000, Thailand. ⁴Research and Innovation Cluster for Natural Health Products, Naresuan University, Phitsanulok-65000, Thailand

*Corresponding author: Tasana Pitaksuteepong; *Email: tasana@nu.ac.th

Received: 20 Jan 2026, Revised and Accepted: 26 May 2026

ABSTRACT

Objective: Cannabidiol (CBD) is a non-psychoactive phytocannabinoid with broad therapeutic potential. However, its extremely poor aqueous solubility limits pharmaceutical development. This study aimed to enhance CBD solubility using binary and ternary amorphous solid dispersions (SDs) prepared by freeze-drying.

Methods: Freeze-drying conditions were optimized by screening solvent systems based on frozen-state thermal behavior. Binary SDs were prepared with polyvinylpyrrolidone (PVP-K30 or PVP-K90), while ternary SDs incorporated surfactants (TPGS, poloxamer 188, and poloxamer 407). Formulations were evaluated for solubility, dissolution, solid-state properties (DSC, FTIR), and stability.

Results: The optimal solvent system was 35% (v/v) tert-butyl alcohol. Binary SDs increased CBD solubility by up to 32-fold. Initial screening of ternary systems achieved approximately 7,000-fold enhancement, with poloxamer 407 showing the greatest effect. Further optimization yielded formulations (F7 and F14) with up to ~11,000-fold increased solubility and rapid dissolution. DSC confirmed complete amorphization, while FTIR indicated intermolecular interactions. The optimized formulations maintained amorphous characteristics and >96% CBD content after six months.

Conclusion: Freeze-dried ternary SDs, particularly those containing poloxamer 407, provide a robust strategy for markedly enhancing CBD solubility and dissolution with good stability.

Keywords: Cannabidiol, Solid dispersion, Freeze-drying, Solubility enhancement, Amorphous system

© 2026 The Authors. Published by Innovare Academic Sciences Pvt Ltd. This is an open access article under the CC BY license (<https://creativecommons.org/licenses/by/4.0/>) DOI: <https://dx.doi.org/10.22159/ijap.2026v18i4.58197> Journal homepage: <https://innovareacademics.in/journals/index.php/ijap>

INTRODUCTION

Cannabidiol (CBD), a major non-psychoactive phytocannabinoids derived from hemp (*Cannabis sativa* L. *subsp. sativa*), has gained significant attention due to its broad pharmacological activities, including neuroprotective, anti-inflammatory, and analgesic effects [1, 2]. Clinically, CBD is approved as an antiepileptic agent (Epidiolex®) [3], and its therapeutic potential has led to increasing interest in pharmaceutical, nutraceutical, and cosmetic applications.

Despite these advantages, CBD exhibits extremely low aqueous solubility (~0.0627 µg/ml [4]) and is classified as a Biopharmaceutics Classification System (BCS) Class II compound. This poor solubility limits its dissolution and oral bioavailability, posing a major challenge for formulation development.

Various formulation strategies have been explored to overcome this limitation, particularly lipid-based systems such as nanoemulsions, microemulsions, and self-emulsifying drug delivery systems (SEDDS) [5-9]. While these approaches can enhance solubilization, they often involve complex compositions and may exhibit variability in drug absorption due to physiological factors [10].

Solid dispersion (SD) systems represent an alternative and effective approach for improving the solubility, dissolution, and bioavailability of poorly water-soluble drugs [4, 11-13]. In these systems, a hydrophobic drug is dispersed within a hydrophilic polymer matrix, enhancing dissolution through improved wettability, reduced particle size, and transformation to an amorphous state. However, the amorphous form is thermodynamically unstable and prone to recrystallization during storage [14].

These limitations can be mitigated through appropriate selection of carrier materials and formulation strategies [15, 16]. In particular, ternary solid dispersions (TSDs), which incorporate a polymer and a surfactant, have been shown to further enhance solubilization and improve physical stability by combining polymer-based stabilization with surfactant-mediated effects [17, 18].

Therefore, the present study aimed to develop and characterize binary and ternary amorphous solid dispersions of CBD using a freeze-drying technique to enhance solubility, dissolution, and solid-state stability. A key feature of this work is the application of frozen-state differential scanning calorimetry (DSC) for solvent system optimization, along with a systematic comparison of binary and ternary systems to elucidate the role of surfactants in enhancing CBD performance.

MATERIALS AND METHODS

Chemicals and reagents

Cannabidiol (CBD; crystalline solid, 99% purity) was obtained from Salus Bioceutical (Thailand) Co., Ltd. (Chiang Mai, Thailand). Polyvinylpyrrolidone (PVP) with two different molecular weights—PVP-K30 (Mw ≈ 40,000 g/mol) and PVP-K90 (Mw ≈ 360,000 g/mol)—was purchased from Tokyo Chemical Industry Co., Ltd. (Tokyo, Japan) and used as polymeric carriers. Three surfactants, namely d-α-tocopheryl polyethylene glycol 1000

succinate (TPGS), poloxamer 188 (P188), and poloxamer 407 (P407), were obtained from Chanjao Longevity Co., Ltd. (Bangkok, Thailand). Ethanol (99.9%, AR grade), tert-butyl alcohol (t-BA, AR grade), acetonitrile (AR grade), and ultra-pure water (18 M Ω . cm) were used as solvents during formulation. Ammonium formate (98%, AR grade), formic acid (98%, AR grade), and acetonitrile (HPLC grade) were used for preparation of the HPLC mobile phase.

Instruments

The following instruments were used in this study: a Gamma 2-16 ISC plus freeze-dryer (Martin Christ Gefriertrocknungsanlagen GmbH, Osterode am Harz, Germany); differential scanning calorimeters DSC1 and DSC5+ (Mettler-Toledo AG, Greifensee, Switzerland); a 1260 Quat Pump VL high-performance liquid chromatography system (Agilent Technologies, Santa Clara, CA, USA); a Spectrum 400 Fourier transform infrared spectrometer (PerkinElmer Inc., Waltham, MA, USA); and a DSA25 drop-shape analyzer (KRÜSS GmbH, Hamburg, Germany).

Methods

Optimization of the preparation process for CBD solid dispersions

CBD solid dispersions were prepared by dissolving CBD and polymeric carriers in appropriate solvent systems, followed by solvent removal using freeze-drying. Selection of a solvent system capable of dissolving both CBD and PVP while remaining in a solid-state during freeze-drying was a critical step.

Binary CBD solid dispersions were initially prepared using PVP-K30 or PVP-K90 as carriers, with CBD loading fixed at 20% w/w relative to the polymer. Three organic solvents—ethanol, acetonitrile, and tert-butyl alcohol—were evaluated at various solvent-to-water ratios (0–100% v/v). Solvent systems were considered suitable if they could be completely frozen after storage at -80 °C for 24 h. Selected solvent systems were further assessed for their ability to fully dissolve CBD and PVP prior to freeze-drying.

Differential scanning calorimetry (DSC; Mettler-Toledo DSC 5+) was used to assess the thermal behavior of frozen CBD/PVP solutions by modifying a previously published technique [19]. Approximately 5–8 mg of each sample was sealed in aluminum pans to prevent solvent evaporation. Samples were cooled from 25 °C to -80 °C at a rate of 10 °C/min, held for 5 min, and reheated to 25 °C at 5 °C/min under a nitrogen purge of 50 ml/min.

Preparation of CBD binary solid dispersions (CBD-BSDs)

CBD-BSDs containing 20% w/w CBD were prepared using either PVP-K30 or PVP-K90. CBD and the polymer were separately dissolved in the selected organic solvent and ultra-pure water, respectively, to achieve the optimized solvent-to-water ratio. The two solutions were then combined and stirred until complete dissolution was achieved [20].

The resulting solutions were frozen at -80 °C and subsequently freeze-dried using a Gamma 2-16 ISC plus freeze-dryer equipped with a drying manifold suitable for organic solvents. The freeze-drying conditions were as follows: condenser temperature -80 °C, shelf temperature -40 °C, and chamber pressure 0.128 mbar (96 mTorr). The dried solid dispersions were gently ground and stored in a desiccator at room temperature until further analysis.

Preparation of CBD ternary solid dispersions (CBD-TSDs)

CBD-TSDs were prepared using a procedure similar to that of the binary systems, with the addition of a surfactant as the third component. During the initial surfactant screening step, the carrier system consisted of PVP and surfactant at a fixed weight ratio of 65:15, while the overall carrier-to-drug ratio was maintained at 4:1 (i. e., 20% CBD, 65% PVP, and 15% surfactant). Three surfactants, including TPGS, P188, and P407, were evaluated based on their ability to enhance CBD solubility.

Following selection of the most suitable surfactant, formulation optimization was performed by varying the CBD content (10%, 15%, and 20% w/w) and the surfactant proportion (15%, 20%, and 30% w/w), with PVP comprising the remaining percentage of the formulation. All formulations were prepared using the optimized solvent system and freeze-drying conditions described above.

HPLC analysis of CBD

CBD content was quantified using an Agilent 1260 Infinity II HPLC system following the method described by Jaidee *et al.* [21]. Chromatographic separation was achieved using a Phenomenex Kinetex C18 column (2.6 μ m, 4.6 \times 150 mm). The mobile phase consisted of acetonitrile and 20 mmol ammonium formate buffer (pH 3.6) in a 75:25 (v/v) ratio. The flow rate was set at 0.8 ml/min, the column temperature was maintained at 40 °C, and detection was performed at 220 nm. The injection volume was 5 μ l. Calibration curves were constructed using CBD standard solutions over the concentration range of 2.5–50 μ g/ml. All analyses were performed in triplicate.

Characterization of solid dispersions

Yield and CBD content

The percentage yield of the solid dispersions was calculated using the following equation [22]:

$$\text{Yield (\%)} = \frac{\text{Weight of dried solid dispersion}}{\text{Total weight of CBD and carriers}} \times 100$$

To determine CBD content, each solid dispersion was accurately weighed and dissolved in methanol to obtain a concentration of 1 mg/ml. The solution was stirred for 5 min, filtered, and appropriately diluted prior to HPLC analysis. CBD content was calculated as [22]:

$$\text{CBD content (\%)} = \frac{\text{Measured CBD content}}{\text{Theoretical CBD content}} \times 100$$

Saturated solubility study

The saturated solubility of CBD from solid dispersions was determined using a modification of a previously described method [23]. An excess amount of each formulation was dispersed in 6 ml of ultra-pure water (18 M Ω .cm) and stirring at 100 rpm for 24 h at 25 \pm 2 °C to ensure equilibrium. The suspensions were then centrifuged at 15,000 rpm for 30 min at 25 °C, and the supernatant was filtered through a 0.22 μ m nylon membrane filter. The concentration of dissolved CBD in the filtrate was quantified by HPLC.

Differential scanning calorimetry (DSC) analysis

Thermal properties and solid-state characteristics were examined using DSC (Mettler-Toledo DSC1). Approximately 2–3 mg of each sample was sealed in aluminum pans and heated from 25 °C to 250 °C at a rate of 10 °C/min under a nitrogen flow of 50 ml/min. Thermograms were compared with those of pure CBD and excipients to assess amorphization.

Fourier transform infrared (FTIR) spectroscopy analysis

Attenuated total reflection-Fourier transform infrared (ATR-FTIR) spectroscopy was used to investigate potential intermolecular interactions between CBD and carriers. ATR-FTIR spectra were recorded using a Perkin Elmer Spectrum 400 spectrophotometer. Samples included pure CBD, individual carriers, physical mixtures, and optimized binary and ternary solid dispersions. Spectra were collected over the range of 4000–400 cm^{-1} with a resolution of 8 cm^{-1} [24].

Contact angle measurement

Contact angle measurements were performed to evaluate wettability using a DSA25 drop-shape analyzer based on the sessile drop method [25]. Powder samples (150 mg) were compressed into flat discs (13 mm diameter) using a hydraulic press at a pressure of 2 tons for 15 s. After calibration, a 10 μl droplet of deionized water was deposited onto the disc surface. Static images were captured immediately, and contact angles were determined using image analysis software based on Young-Laplace fitting [26]. Measurements were conducted in triplicate at room temperature.

In vitro dissolution

In vitro dissolution studies were conducted as a comparative, non-compendial assessment by dispersing the optimized CBD solid dispersions in ultra-pure water at concentrations of 0.1 mg/ml and 0.75 mg/ml, with continuous stirring at 100 rpm at 25 ± 2 °C.

The concentration of 0.1 mg/ml of formulation corresponds to approximately 10 $\mu\text{g/ml}$ of CBD and was selected to represent sink conditions, defined as $\leq 10\%$ of the equilibrium solubility of CBD in the dissolution medium. Based on the measured saturated solubility (~ 600 – 660 $\mu\text{g/ml}$), this condition satisfies commonly accepted sink criteria.

In contrast, the 0.75 mg/ml condition (equivalent to 75 $\mu\text{g/ml}$ CBD) was selected to simulate practical application scenarios, consistent with regulatory limits permitting CBD concentrations of up to 75 ppm ($\mu\text{g/ml}$) in food and beverage products.

At predetermined time points (3, 5, 10, 15, 30, 60, 90, 120, and 360 min), aliquots were withdrawn, filtered, diluted as necessary, and analyzed by HPLC. Each experiment was performed in triplicate.

Stability testing

Optimized CBD solid dispersions were subjected to long-term stability testing under ambient storage conditions. Samples were stored in tightly closed glass vials and placed in a desiccator with newly regenerated silica gel. The storage temperature was maintained at ambient laboratory conditions (30 ± 2 °C) for 6 mo. Then, they were analyzed for chemical and physical stability. CBD content was quantified using a validated HPLC method, and solid-state characteristics were evaluated by DSC to monitor potential recrystallization. All measurements were performed in triplicate.

Statistical analysis

Statistical analysis was performed using one-way analysis of variance (ANOVA), followed by Scheffé's or Games-Howell's post hoc tests, as appropriate. A significant level of $p < 0.05$ was applied. Statistical analyses were performed using SPSS Statistics version 17.0 (IBM Corp., Armonk, NY, USA).

RESULTS AND DISCUSSION

Rationale for polymer selection

Polyvinylpyrrolidone (PVP) was selected as the carrier polymer due to its high solubility in aqueous and organic media and its compatibility with poorly water-soluble drugs [27]. Its hydrophilic nature improves drug wettability, while its relatively high glass transition temperature (T_g) can reduce molecular mobility and contribute to stabilization of the amorphous drug [11, 28, 29]. In addition, PVP is capable of forming intermolecular interactions, particularly hydrogen bonding, which may inhibit recrystallization and enhance solubility and dissolution [30].

These properties are particularly relevant for freeze-dried systems, where the T_g of the matrix plays a critical role in maintaining structural integrity and preventing collapse during processing and storage.

To investigate the influence of polymer characteristics, two grades of PVP with different molecular weights, PVP-K30 and PVP-K90, were selected, as both have demonstrated favorable performance in solid dispersion systems [31]. This comparison enables evaluation of the impact of polymer chain length on molecular mobility, drug-polymer interactions, and overall formulation performance.

Solvent system selection for freeze-drying

Freeze-drying was selected as the solvent removal technique for preparing CBD solid dispersions due to its suitability for thermolabile compounds and its ability to produce highly porous matrices that enhance dissolution while minimizing drug degradation and processing losses [32]. The freezing behavior of the solvent system is critical, as it governs frozen-matrix formation and influences the risk of collapse during drying [33, 34].

Solvent selection was based on two criteria: complete solubilization of CBD and polymer prior to freezing, and suitable frozen-state thermal properties. Ethanol, acetonitrile, and tert-butyl alcohol (t-BA) were evaluated at different compositions. A 20% (w/w) CBD/PVP-K90 formulation was used as a model system during solvent screening. Because PVP-K90 has the same chemical structure as PVP-K30 but lower solubility due to its higher molecular weight, solvent systems capable of dissolving PVP-K90 were considered suitable for PVP-K30-based formulations.

Ethanol-based systems could be completely frozen only at concentrations up to 80% v/v, whereas acetonitrile- and t-BA-based systems remained frozen across all tested concentrations (fig. 1). However, complete solubilization of both CBD and PVP-K90 was achieved only at specific solvent compositions (fig. 2). Based on these results, solvent systems containing 45% v/v ethanol, 45% v/v acetonitrile, and 35% v/v t-BA were selected for frozen-state thermal analysis to support freeze-drying process optimization.

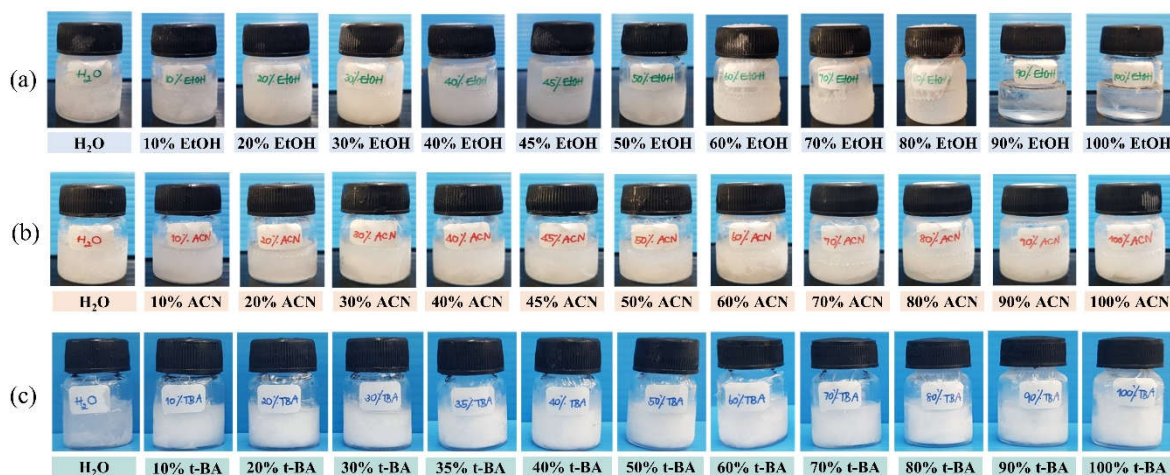


Fig. 1: Physical appearance of frozen samples prepared using (a) ethanol (EtOH), (b) acetonitrile (ACN), and (c) tert-butyl alcohol (t-BA) aqueous systems at varying solvent concentrations (0–100% v/v) after freezing at -80 °C. The solvent composition increases from left to right in each panel

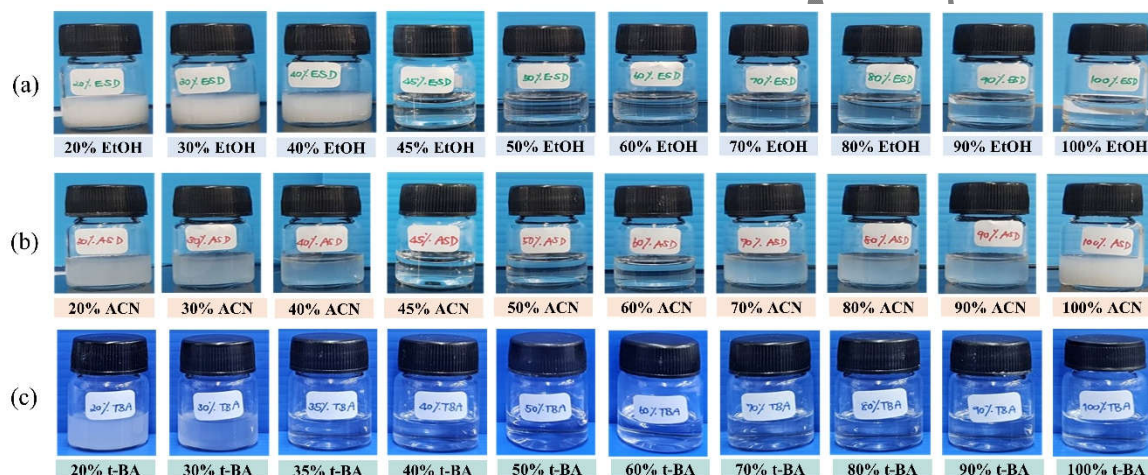


Fig. 2: Physical appearance of solutions containing CBD and PVP-K90 (20% CBD/80% PVP-K90) in (a) ethanol (EtOH), (b) acetonitrile (ACN), and (c) tert-butyl alcohol (t-BA) aqueous systems at varying solvent concentrations (20–100% v/v). The solvent composition increases from left to right in each panel

Thermal analysis of frozen CBD/PVP solutions

Differential scanning calorimetry (DSC) was employed to investigate the frozen-state behavior and identify systems with minimal phase separation. The ethanol-based system exhibited a single exothermic peak at approximately -57 to -58 °C, indicating a relatively uniform freezing event (fig. 3a, thermograms (i) and (ii)). However, upon reheating, minor endothermic transitions were observed at -54 to -56 °C and -40 to -41 °C, corresponding to melting of ethanol-rich and water-rich phases, respectively [19] (fig. 3b, thermograms (i) and (ii)). These features suggest partial phase separation during freezing, which may compromise frozen-matrix uniformity and increase the risk of structural instability during primary drying.

Acetonitrile-based system exhibited more complex thermal behavior, with two distinct exothermic peaks during cooling and multiple endothermic transitions during reheating (fig. 3). This behavior indicates phase separation between acetonitrile-rich and water-rich domains [35], which is undesirable due to increased collapse risk and nonuniform drying.

In contrast, the t-BA-based system exhibited single, well-defined exothermic events during cooling at higher onset temperatures (-26 to -29 °C) (fig. 3), consistent with the relatively high freezing point of t-BA and its weaker hydrogen-bonding interactions with water [36, 37]. The corresponding heating curves displayed sharp endothermic peaks at approximately -8 °C, attributed to the melting of a t-BA hydrate-water complex [38]. These consistent single-phase thermal transitions indicate formation of a homogeneous frozen matrix with a clearly defined collapse-related temperature, suggesting favorable suitability for freeze-drying.

DSC analysis demonstrated that t-BA-based systems produced the most stable frozen matrix. Visual inspection of the freeze-dried products supported these findings (fig. 4), with t-BA-based formulations yielding well-formed, sponge-like cakes, whereas ethanol- and acetonitrile-based systems exhibited partial collapse or surface drug separation.

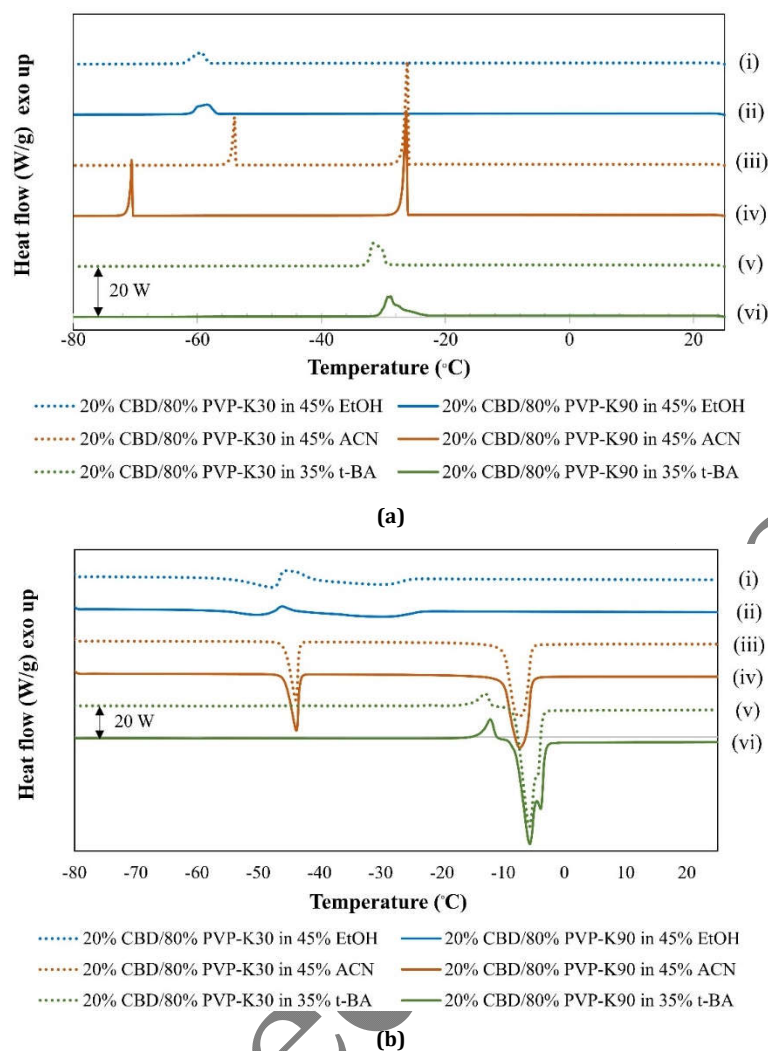


Fig. 3: DSC thermograms of (i) 20% CBD/80% PVP-K30 in 45% ethanol, (ii) 20% CBD/80% PVP-K90 in 45% ethanol, (iii) 20% CBD/80% PVP-K30 in 45% acetonitrile, (iv) 20% CBD/80% PVP-K90 in 45% acetonitrile, (v) 20% CBD/80% PVP-K30 in 35% tert-butyl alcohol, and (vi) 20% CBD/80% PVP-K90 in 35% tert-butyl alcohol during (a) the cooling process (from 25 °C to -80 °C at a rate of 10 °C/min) and (b) the heating process (from -80 °C to 25 °C at a rate of 5 °C/min)



Fig. 4: Appearance of freeze-dried products prepared from binary solid dispersions containing 20% CBD and 80% polymer (PVP-K30 or PVP-K90) using different solvent systems: (a) 45% ethanol, (b) 45% acetonitrile, and (c) 35% tert-butyl alcohol. Corresponding formulations with PVP-K30 and PVP-K90 are shown for each solvent condition

CBD binary and ternary solid dispersions

Yield and CBD content

All formulations exhibited high yield and drug content, indicating efficient processing and minimal drug loss (table 1). The incorporation of surfactants did not adversely affect CBD content, confirming good compatibility between CBD and the excipients.

Table 1: Percentage yield, CBD content, and saturated solubility of CBD solid dispersions prepared during the initial screening stage, including (a) the binary systems and (b) the ternary systems with various types of surfactants, using 35% (v/v) tert-butyl alcohol (t-BA) as the solvent

Formulations	% Yield	CBD content	Solubility of CBD ($\mu\text{g/ml}$)	Fold increase
Pure CBD	-	-	0.06	-
(a) Binary system				
20% CBD/80% PVP-K30	97.14 \pm 1.70	97.62 \pm 3.87	1.27 \pm 0.45 ^a	21.24
20% CBD/80% PVP-K90	95.23 \pm 1.61	97.19 \pm 2.14	1.94 \pm 0.16 ^a	32.38
(b) Ternary system with various surfactants				
20% CBD/65% PVP-K30/15% TPGS	97.37 \pm 0.29	94.66 \pm 1.49	12.06 \pm 1.63 ^b	200.92
20% CBD/65% PVP-K30/15% P188	99.01 \pm 0.33	98.67 \pm 1.34	12.79 \pm 1.87 ^b	213.14
20% CBD/65% PVP-K30/15% P407 [†]	99.30 \pm 0.25	99.41 \pm 4.22	390.60 \pm 20.90 ^c	6,510.08
20% CBD/65% PVP-K90/15% TPGS	98.22 \pm 0.38	98.91 \pm 1.93	20.54 \pm 2.89 ^b	342.34
20% CBD/65% PVP-K90/15% P188	99.09 \pm 0.26	99.06 \pm 0.76	13.72 \pm 0.56 ^b	228.66
20% CBD/65% PVP-K90/15% P407 [†]	99.68 \pm 0.65	98.56 \pm 1.35	419.31 \pm 8.15 ^c	6,988.46

Note: Results are presented as mean \pm SD. Sample size was $n = 3$ for all formulations unless otherwise indicated; formulations marked with \dagger were analyzed with $n = 4$. Means not sharing a letter differ significantly ($p < 0.05$, Games-Howell test, 95% confidence interval). Fold increase was calculated relative to pure CBD solubility in Milli-Q water (0.0627 $\mu\text{g/ml}$) [4].

Solubility enhancement

CBD concentrations were quantified using a validated HPLC method in accordance with ICH Q2 guidelines [39]. The calibration curve demonstrated excellent linearity over the concentration range of 2.5–50 $\mu\text{g/ml}$ ($r^2 = 0.9999$). The limits of detection (LOD) and quantification (LOQ) were 0.08 $\mu\text{g/ml}$ and 2.41 $\mu\text{g/ml}$, respectively.

Binary solid dispersions markedly improved CBD solubility compared with crystalline CBD (table 1). This enhancement is attributable to amorphization of CBD and improved wettability imparted by the hydrophilic polymer matrix [40]. These findings are consistent with previous reports on PVP-based CBD solid dispersions [4, 41].

Further enhancement was observed in ternary systems, particularly those containing poloxamer 407, which showed the strongest solubilization effect during the initial screening stage (table 1). The effect is primarily attributed to micellar solubilization and reduction of interfacial tension, which facilitate improved drug–water interactions [28].

TPGS forms micelles with a hydrophobic tocopherol succinate core and a hydrophilic polyethylene glycol shell, while P188 and P407 form with polypropylene oxide (PPO) cores and polyethylene oxide (PEO) coronas above their critical micelle concentration (CMC) [42, 43]. Du Noüy ring tensiometry (supplementary fig. S1 and table S1) showed that P407 had the lowest CMC, followed by TPGS and P188, indicating more efficient micelle formation at lower concentrations. This property likely contributes to the superior solubilization performance of P407, consistent with previous reports [44, 45].

Effect of formulation ratios on solubility

Formulation composition significantly influenced solubility performance (table 2). Systems containing PVP-K90 consistently exhibited higher solubility than those containing PVP-K30, likely due to stronger drug–polymer interactions and enhanced molecular immobilization.

Increasing surfactant content improved solubility up to an optimal level, confirming the synergistic effect between polymer and surfactant. However, excessive surfactant did not result in proportional improvement. This behavior may be attributed to excessive surfactant disrupting the polymer–drug interaction network within the solid dispersion matrix. Elevated surfactant concentrations may weaken matrix integrity, alter local viscosity, and affect micelle packing behavior, thereby reducing stabilization of the amorphous drug and promoting partial phase separation.

Reducing drug loading further enhanced solubility, likely due to improved molecular dispersion within the carrier matrix. Formulations F7 and F14 were identified as optimal systems.

Table 2: Saturated solubility and fold enhancement of CBD in optimized ternary solid dispersion formulations (CBD-TSD; F1–F14) with varying ratios of cannabidiol (CBD), polyvinylpyrrolidone (PVP), and poloxamer 407 (P407), measured in aqueous solution

Code	Formulations	Drug/carrier ratio CBD: PVP: P407	Solubility of CBD ($\mu\text{g/ml}$)	Fold increase
CBD-TSD products with PVP-K30				
F1	20% CBD/65% PVP-K30/15% P407	20: 65: 15	390.60 \pm 20.90 ^{c,d,e}	6,510.08
F2	20% CBD/60% PVP-K30/20% P407	20: 60: 20	622.58 \pm 18.55 ^e	10,376.39
F3	20% CBD/50% PVP-K30/30% P407	20: 50: 30	224.75 \pm 20.38 ^a	3,745.80
F4	15% CBD/55% PVP-K30/30% P407 [†]	15: 55: 30	438.49 \pm 12.96 ^{e,f}	7,308.14
F5	10% CBD/75% PVP-K30/15% P407	10: 75: 15	197.51 \pm 9.23 ^a	3,291.78
F6	10% CBD/70% PVP-K30/20% P407 [†]	10: 70: 20	321.09 \pm 21.52 ^{b,c}	5,351.42
F7	10% CBD/60% PVP-K30/30% P407 [†]	10: 60: 30	606.21 \pm 15.20 ^e	10,103.46
CBD-TSD products with PVP-K90				
F8	20% CBD/65% PVP-K90/15% P407	20: 65: 15	419.31 \pm 8.15 ^{d,e}	6,988.46
F9	20% CBD/60% PVP-K90/20% P407	20: 60: 20	632.45 \pm 8.37 ^e	10,540.91
F10	20% CBD/50% PVP-K90/30% P407	20: 50: 30	353.10 \pm 25.19 ^{c,d}	5,884.99
F11	15% CBD/55% PVP-K90/30% P407 [†]	15: 55: 30	506.11 \pm 24.57 ^f	8,435.18
F12	10% CBD/75% PVP-K90/15% P407	10: 75: 15	252.68 \pm 21.38 ^{a,b}	4,211.31

F13	10% CBD/70% PVP-K90/20% P407 [†]	10: 70: 20	414.09 ± 36.10 ^{d,e}	6,901.47
F14	10% CBD/60% PVP-K90/30% P407 [‡]	10: 60: 30	660.46 ± 16.86 ^g	11,007.74

Note: Results are presented as mean ± SD. Sample size was $n = 4$ for all formulations unless otherwise indicated. Formulations marked with [†] were analyzed with $n = 3$, and those marked with [‡] were analyzed with $n = 5$. Means not sharing a letter differ significantly ($p < 0.05$, Scheffé's test, 95% confidence interval). Fold increase was calculated relative to pure CBD solubility in Milli-Q water (0.0627 $\mu\text{g/ml}$) [4].

Amorphization assessment of the optimized formulations by DSC

DSC analysis confirmed the absence of the characteristic melting peak of crystalline CBD in the optimized formulations (fig. 5), indicating complete amorphization and effective molecular dispersion. This behavior can be attributed to the combined effects of PVP as a crystallization inhibitor and P407 as a molecular dispersant, which together stabilize CBD in an amorphous state by restricting molecular mobility and preventing recrystallization [11].

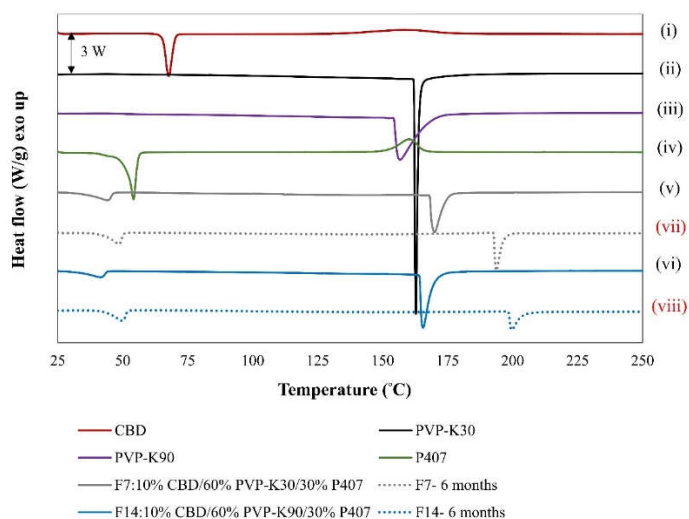


Fig. 5: Differential scanning calorimetry (DSC) thermograms of (i) pure CBD, (ii) PVP-K30, (iii) PVP-K90, and (iv) poloxamer 407 (P407), along with ternary solid dispersion formulations: (v) F7 (10% CBD/60% PVP-K30/30% P407) and (vi) F14 (10% CBD/60% PVP-K90/30% P407). Thermograms of stability samples after six months of storage are also shown: (vii) F7 after 6 mo and (viii) F14 after 6 mo

FTIR analysis

FTIR spectroscopy indicated intermolecular interactions between CBD and formulation components, primarily through hydrogen bonding, which contributes to stabilization of the amorphous form.

Pure CBD exhibited characteristic absorption bands at 2922 cm^{-1} (CH_3/CH_2 stretching), 1213 cm^{-1} (C–O stretching), and a broad O–H stretching region between 3406 and 3517 cm^{-1} corresponding to free and hydrogen-bonded hydroxyl groups (fig. 6). PVP-K30 and PVP-K90 displayed prominent carbonyl (C=O) stretching peaks at approximately 1655 and 1660 cm^{-1} , respectively, while P407 showed characteristic CH_2 stretching at $\sim 2880\text{ cm}^{-1}$ and C–O–C stretching at $\sim 1096\text{ cm}^{-1}$.

In both binary and ternary solid dispersions, the O–H stretching band of CBD (3517 cm^{-1}) was disappeared, whereas it remained in physical mixtures. This disappearance indicates the hydrogen bonding between CBD and excipients.

Additionally, slight shifts in the PVP carbonyl stretching band were observed, with peaks shifting to approximately 1653 cm^{-1} in PVP-K30 systems and 1650 – 1651 cm^{-1} in PVP-K90 systems. These shifts suggest the formation of hydrogen bonding interactions between CBD and PVP, with the greater shift in PVP-K90-based formulations indicating stronger interactions. This is consistent with the enhanced solubility and stability observed for these systems.

Although each pyrrolidone unit in PVP contains both carbonyl and nitrogen functionalities, steric hindrance limits the accessibility of the nitrogen atom, making the carbonyl group the primary hydrogen bond acceptor [46]. Furthermore, no distinct absorption band was observed in the region around 2070 cm^{-1} in either pure CBD or the solid dispersions, indicating that no additional interactions or structural changes associated with this region were evident under the present conditions. These findings support the role of hydrogen bonding between CBD and polymeric carriers in stabilizing the amorphous form and contributing to the improved solubility of the developed solid dispersions, in agreement with previous reports [47].

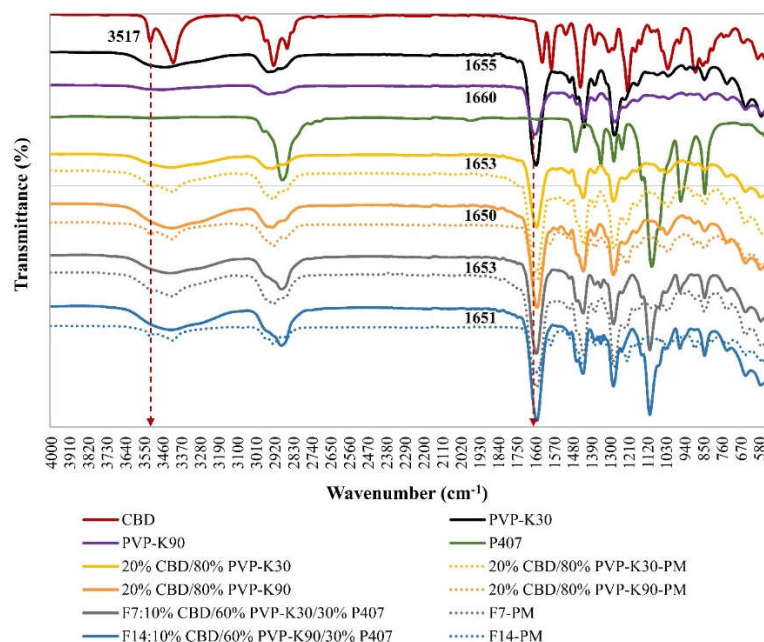


Fig. 6: FTIR spectra of raw materials (pure CBD, PVP-K30, PVP-K90, and P407) and CBD solid dispersions. Binary systems include 20% CBD/80% PVP-K30 and 20% CBD/80% PVP-K90, while ternary systems include F7 (10% CBD/60% PVP-K30/30% P407) and F14 (10% CBD/60% PVP-K90/30% P407). Solid lines represent solid dispersions, and dashed lines represent corresponding physical mixtures (PM)

Contact angle

Contact angle measurements were performed to assess wettability, as lower values indicate improved water penetration and dissolution.

Pure CBD exhibited the highest contact angle, reflecting poor wettability (table 3). Incorporation of PVP in binary formulations significantly reduced contact angles due to its hydrophilic nature, with further reduction observed upon addition of P407 in ternary systems, likely due to decreased interfacial tension.

Reducing CBD content from 20% to 10% further improved wettability, while formulations containing PVP-K30 showed slightly lower contact angles than those with PVP-K90, suggesting a minor effect of polymer molecular weight.

Although the optimized ternary formulations showed markedly improved wettability compared with pure CBD, the measured values indicate that the system remains moderately hydrophobic. This observation suggests that while incorporation of hydrophilic polymers and surfactants significantly improves surface wettability, the intrinsic hydrophobic nature of CBD still influences to the overall surface characteristics of the formulation.

Table 3: The contact angle of water on pure CBD and the prepared formulations in a binary system and four formulations with various CBD content in the ternary systems containing 30%P407 with PVP-K90 or PVP-K30

Formulations	Contact angle (°)		
	1 s	3 s	5 s
Pure CBD	107.67±0.55	105.77±0.55	105.37±0.57
20% CBD/80% PVP-K90	90.97±0.67	88.33±1.37	87.27±0.65
20% CBD/50% PVP-K90/30% P407	71.87±0.47	70.10±0.14	69.35±0.35
15% CBD/55% PVP-K90/30% P407	62.20±0.35	61.17±0.40	60.30±0.26
10% CBD/60% PVP-K90/30% P407	53.53±0.25	52.17±0.35	50.90±0.10
10% CBD/60% PVP-K30/30% P407	41.73±0.21	40.43±0.15	39.47±0.21

Note: Results are presented as mean±SD. Sample size was n = 3 for all formulations.

In vitro dissolution of optimized formulations

In vitro dissolution studies were performed to compare the dissolution performance of the optimized ternary solid dispersions with crystalline CBD. Dissolution profiles of pure CBD and formulations F7 and F14 were assessed at CBD-equivalent concentrations of approximately 10 and 75 µg/ml (corresponding to 0.1 and 0.75 mg/ml of CBD-TSD powder), as shown in fig. 7.

The lower concentration (0.1 mg/ml) represented sink conditions, corresponding to ≤10% of the equilibrium solubility of CBD, ~606–660 µg/ml), ensuring dissolution was not solubility-limited. The higher concentration (0.75 mg/ml) was selected to reflect application-relevant conditions, consistent with regulatory limits for CBD in beverage products [48]. Due to the extremely low aqueous solubility of crystalline CBD, true sink conditions could not be achieved for the pure drug. Therefore, its dissolution behavior was evaluated under non-sink conditions for comparison.

Pure CBD exhibited negligible dissolution, consistent with its hydrophobic nature and poor wettability. In contrast, both F7 and F14 demonstrated rapid and markedly enhanced dissolution under all conditions, attributable to amorphization, improved wettability, and surfactant-mediated solubilization.

Under sink conditions, both formulations exhibited rapid initial dissolution, with more than half of the drug released within the first few minutes, followed by a gradual plateau. At the higher concentration, near-complete dissolution was achieved and maintained throughout the study. These results indicate that the optimized ternary systems provide efficient dissolution across both ideal and application-relevant conditions.

A slight difference in early-stage dissolution was observed, with F14 (PVP-K90) showing marginally slower initial release than F7 (PVP-K30). This behavior is likely due to the higher molecular weight and viscosity of PVP-K90, which may retard diffusion. Nevertheless, both formulations achieved substantial and sustained dissolution enhancement, confirming the effectiveness of the ternary solid dispersion system.

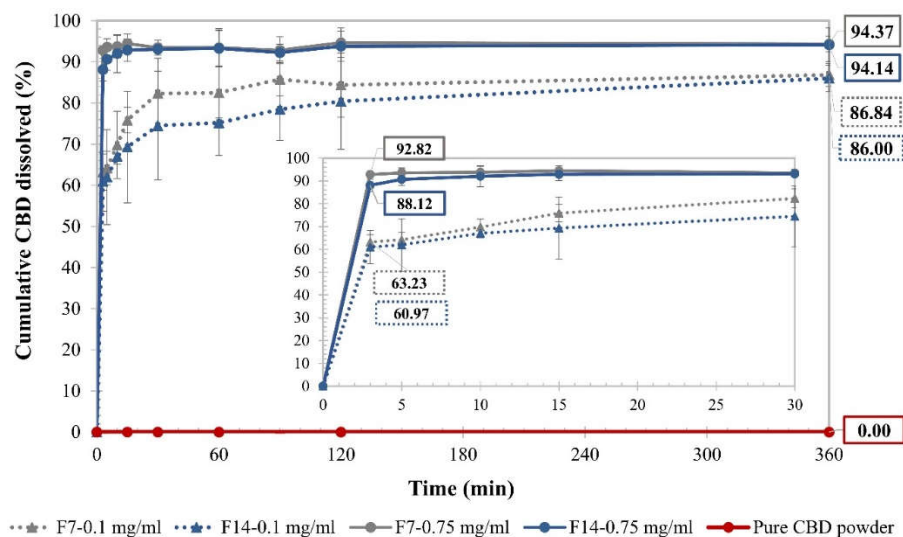


Fig. 7: Dissolution profiles of pure CBD powder and optimized ternary solid dispersions: F7 (10% CBD/60% PVP-K30/30% P407) and F14 (10% CBD/60% PVP-K90/30% P407) in ultra-pure water. F7 is shown in grey and F14 in blue. Dashed lines represent dissolution at 0.1 mg/ml, while solid lines represent 0.75 mg/ml. Pure CBD is shown as a solid red line. The inset highlights the initial dissolution stage

Solid-state stability of optimized CBD solid dispersions

Long-term stability of the optimized freeze-dried formulations was evaluated over six months to assess maintenance of the amorphous state and chemical integrity of CBD. Since the intended storage condition for the developed formulation is refrigerated, storage at ambient temperature (30 ± 2 °C) represents a thermally stressed condition relative to the recommended storage temperature, although the samples were maintained in a desiccator to control moisture exposure.

DSC thermograms of F7 (PVP-K30) and F14 (PVP-K90) showed no evidence of recrystallization, throughout the study period (fig. 5(vii), 5(viii)), confirming preservation of the amorphous structure. This stability is attributed to the formation of a homogeneous amorphous matrix during freeze-drying, which reduces molecular mobility and suppresses recrystallization.

F14 exhibited slightly greater stability than F7, likely due to stronger drug–polymer interactions and enhanced molecular immobilization associated with the higher molecular weight and T_g of PVP-K90 [47]. Additionally, both formulations retained more than 90% of their initial CBD content after six months, indicating good chemical stability.

CONCLUSION

Freeze-dried cannabidiol (CBD) solid dispersions were successfully developed using binary and ternary systems. Optimization of the solvent system identified 35% (v/v) tert-butyl alcohol as suitable for producing a homogeneous matrix during freeze-drying.

Ternary formulations containing polyvinylpyrrolidone and poloxamer 407 significantly enhanced solubility and dissolution compared with binary systems, with F14 (PVP-K90) showing superior overall performance. The optimized formulation achieved up to ~11,000-fold improvement in apparent solubility and exhibited complete amorphization, improved wettability, and maintained physical and chemical stability over six months.

These findings demonstrate that freeze-dried ternary solid dispersions provide an effective strategy for improving the solubility, dissolution, and stability of CBD. This approach may also be applicable to other poorly water-soluble drugs and support the development of pharmaceutical and related products.

ACKNOWLEDGEMENT

The authors gratefully acknowledge the Faculty of Pharmaceutical Sciences, Naresuan University, for providing facilities and instrumental support. The authors also thank Ms. Supaporn Tuanthai, Mr. Phumbodin Chupinidsakulwong, and the technical staff of the Faculty of Pharmaceutical Sciences, Naresuan University, for their valuable technical assistance.

During the preparation of this work, the authors used Grammarly and ChatGPT for language polishing and grammar correction. After using these tools, the authors reviewed and edited the content as needed and took full responsibility for the content of the publication.

FUNDING

This work was partially supported by the Global and Frontier Research University Fund, Naresuan University (Grant No. R2566C053), the Frontier Research and Innovation Cluster Fund, Naresuan University (Grant No. R2569C007), and a scholarship for high-potential students from the Graduate School, Naresuan University.

AUTHORS CONTRIBUTIONS

Thanaporn Juntanon contributed to conceptualization, methodology, investigation, formal analysis, visualization, and writing of the original draft, as well as review and editing of the manuscript. Neti Waranuch contributed to conceptualization, funding acquisition, and co-supervision of the project. Kornkanok Ingkaninan contributed to methodology, particularly the development and validation of the HPLC analytical method for CBD. Tasana Pitaksuteepong contributed to conceptualization, methodology, project administration, supervision, funding acquisition, and writing of the original draft, as well as review and editing of the manuscript. All authors have read and approved the final version of the manuscript.

CONFLICT OF INTERESTS

The authors declare no conflict of interest

REFERENCES

- Atalay S, Jarocka-Karpowicz I, Skrzydlewska E. Antioxidative and anti-inflammatory properties of cannabidiol. *Antioxidants* (Basel). 2019;9(1):21. doi: [10.3390/antiox9010021](https://doi.org/10.3390/antiox9010021), PMID 31881765.
- Cásedas G, Yarza-Sancho MD, López V. Cannabidiol (CBD): a systematic review of clinical and preclinical evidence in the treatment of pain. *Pharmaceuticals* (Basel). 2024;17(11):1438. doi: [10.3390/ph17111438](https://doi.org/10.3390/ph17111438), PMID 39598350.
- Freeman TP, Hindocha C, Green SF, Bloomfield MA. Medicinal use of cannabis based products and cannabinoids. *BMJ*. 2019;365:l1141. doi: [10.1136/bmj.l1141](https://doi.org/10.1136/bmj.l1141), PMID 30948383.
- Koch N, Jennotte O, Gasparini Y, Vandenbroucke F, Lechanteur A, Evrard B. Cannabidiol aqueous solubility enhancement: comparison of three amorphous formulations strategies using different type of polymers. *Int J Pharm*. 2020;589:119812. doi: [10.1016/j.ijpharm.2020.119812](https://doi.org/10.1016/j.ijpharm.2020.119812). PMID 32882367.
- Nakano Y, Tajima M, Sugiyama E, Sato VH, Sato H. Development of a novel nano-emulsion formulation to improve intestinal absorption of cannabidiol. *Med Cannabis Cannabinoids*. 2019;2(1):35-42. doi: [10.1159/000497361](https://doi.org/10.1159/000497361), PMID 34676352.
- Leibtag S, Peshkovsky A. Cannabis extract nanoemulsions produced by high-intensity ultrasound: formulation development and scale-up. *J Drug Deliv Sci Technol*. 2020;60:101953. doi: [10.1016/j.jddst.2020.101953](https://doi.org/10.1016/j.jddst.2020.101953).
- Banerjee A, Binder J, Salama R, Trant JF. Synthesis, characterization and stress-testing of a robust quillaja saponin stabilized oil-in-water phytocannabinoid nanoemulsion. *J Cannabis Res*. 2021;3(1):43. doi: [10.1186/s42238-021-00094-w](https://doi.org/10.1186/s42238-021-00094-w), PMID 34556180.
- Knaub K, Sartorius T, Dharsono T, Wacker R, Wilhelm M, Schön C. A novel self-emulsifying drug delivery system (SEDDS) based on VESIsorb® formulation technology improving the oral bioavailability of cannabidiol in healthy subjects. *Molecules*. 2019;24(16):2967. doi: [10.3390/molecules24162967](https://doi.org/10.3390/molecules24162967), PMID 31426272.
- Taha IE, ElSohly MA, Radwan MM, Elkanayati RM, Wanas A, Joshi PH, et al. Enhancement of cannabidiol oral bioavailability through the development of nanostructured lipid carriers: *in vitro* and *in vivo* evaluation studies. *Drug Deliv Transl Res*. 2025;15(8):2722-32. doi: [10.1007/s13346-024-01766-9](https://doi.org/10.1007/s13346-024-01766-9), PMID 39738884.
- Wang TY, Liu M, Portincasa P, Wang DQ. New insights into the molecular mechanism of intestinal fatty acid absorption. *Eur J Clin Invest*. 2013;43(11):1203-23. doi: [10.1111/eci.12161](https://doi.org/10.1111/eci.12161), PMID 24182389.
- Shirke SH, Shewale SB, Kulkarni AS, Aloorkar NH. Solid dispersion: a novel approach for poorly water soluble drugs. *Int J Curr Pharm Res*. 2015;7(4):1-8.
- Guntaka PR, Lankalapalli S. Solid dispersion – a novel approach for bioavailability enhancement of poorly water-soluble drugs in solid oral dosage forms. *Asian J Pharm Clin Res*. 2019;12(2):17-26. doi: [10.22159/ajpcr.2019.v12i2.29157](https://doi.org/10.22159/ajpcr.2019.v12i2.29157).
- Jennotte O, Koch N, Lechanteur A, Evrard B. Development of amorphous solid dispersions of cannabidiol: influence of the carrier, the hot-melt extrusion parameters and the use of a crystallization inhibitor. *J Drug Deliv Sci Technol*. 2022;71:103372. doi: [10.1016/j.jddst.2022.103372](https://doi.org/10.1016/j.jddst.2022.103372).
- Bhugra C, Pikal MJ. Role of thermodynamic, molecular, and kinetic factors in crystallization from the amorphous state. *J Pharm Sci*. 2008;97(4):1329-49. doi: [10.1002/jps.21138](https://doi.org/10.1002/jps.21138), PMID 17722100.
- Tran P, Pyo YC, Kim DH, Lee SE, Kim JK, Park JS. Overview of the manufacturing methods of solid dispersion technology for improving the solubility of poorly water-soluble drugs and application to anticancer drugs. *Pharmaceutics*. 2019;11(3):132. doi: [10.3390/pharmaceutics11030132](https://doi.org/10.3390/pharmaceutics11030132), PMID 30893899.
- Zhang Z, Dong L, Guo J, Li L, Tian B, Zhao Q, et al. Prediction of the physical stability of amorphous solid dispersions: relationship of aging and phase separation with the thermodynamic and kinetic models along with characterization techniques. *Expert Opin Drug Deliv*. 2020;18(2):249-64. doi: [10.1080/17429247.2021.1844181](https://doi.org/10.1080/17429247.2021.1844181), PMID 33112679.
- Saboo S, Bapat P, Moseson DE, Kestur US, Taylor LS. Exploring the role of surfactants in enhancing drug release from amorphous solid dispersions at higher drug loadings. *Pharmaceutics*. 2021;13(5):735. doi: [10.3390/pharmaceutics13050735](https://doi.org/10.3390/pharmaceutics13050735), PMID 34067666.
- Budiman A, Lailasari E, Nurani NV, Yunita EN, Anastasya G, Aulia RN, et al. Ternary solid dispersions: a review of the preparation, characterization, mechanism of drug release, and physical stability. *Pharmaceutics*. 2023;15(8):2116. doi: [10.3390/pharmaceutics15082116](https://doi.org/10.3390/pharmaceutics15082116), PMID 37631330.
- Koga K, Yoshizumi H. Differential scanning calorimetry (DSC) studies on the structures of water-ethanol mixtures and aged whiskey. *J Food Sci*. 1977;42(5):1213-7. doi: [10.1111/j.1365-2621.1977.tb14462.x](https://doi.org/10.1111/j.1365-2621.1977.tb14462.x).
- Fitriani L, Haq A, Zaini E. Preparation and characterization of solid dispersion freeze-dried efavirenz – polyvinylpyrrolidone K-30. *J Adv Pharm Technol Res*. 2016;7(3):105-9. doi: [10.4103/2231-4040.184592](https://doi.org/10.4103/2231-4040.184592), PMID 27429930, PMCID PMC4932804.
- Jaidee W, Siridechakorn I, Nessopa S, Wisutitprot V, Chaiwangrach N, Ingkaninan K, et al. Kinetics of CBD, Δ⁹-THC degradation and cannabinol formation in cannabis resin at various temperature and pH conditions. *Cannabis Cannabinoid Res*. 2022;7(4):537-47. doi: [10.1089/can.2021.0004](https://doi.org/10.1089/can.2021.0004), PMID 34096805.
- Sapkal SB, Adhao VS, Thenge RR, Darakhe RA, Shinde SA, Shrikhande VN. Formulation and characterization of solid dispersions of etoricoxib using natural polymers. *Turk J Pharm Sci*. 2020;17(1):7-19. doi: [10.4274/tjps.galenos.2018.04880](https://doi.org/10.4274/tjps.galenos.2018.04880). PMID 32454755.
- Almeida H, Ferreira B, Fernandes-Lopes C, Araújo F, Bonifácio MJ, Vasconcelos T, et al. Third-generation solid dispersion through lyophilization enhanced oral bioavailability of resveratrol. *ACS Pharmacol Transl Sci*. 2024;7(3):888-98. doi: [10.1021/acspstsci.4c00029](https://doi.org/10.1021/acspstsci.4c00029), PMID 38481698.
- Possenti E, Colombo C, Realini M, Song CL, Kazarian SG. Time-resolved ATR-FTIR spectroscopy and macro ATR-FTIR spectroscopic imaging of inorganic treatments for stone conservation. *Anal Chem*. 2021;93(44):14635-42. doi: [10.1021/acs.analchem.1c02392](https://doi.org/10.1021/acs.analchem.1c02392). PMID 34699174.
- Bruel C, Queffeuilou S, Darlow T, Virgilio N, Tavares JR, Patience GS. Experimental methods in chemical engineering: contact angles. *Can J Chem Eng*. 2019;97(4):832-42. doi: [10.1002/cjce.23408](https://doi.org/10.1002/cjce.23408).

26. Yuan Y, Lee TR. Contact angle and wetting properties. In: Bracco G, Holst B, editors. Surface science techniques. Berlin, Heidelberg: Springer Berlin Heidelberg. 2013;p. 3-34. doi: [10.1007/978-3-642-34243-1_1](https://doi.org/10.1007/978-3-642-34243-1_1).
27. Luo Y, Hong Y, Shen L, Wu F, Lin X. Multifunctional role of polyvinylpyrrolidone in pharmaceutical formulations. AAPS PharmSciTech. 2021;22(1):34. doi: [10.1208/s12249-020-01909-4](https://doi.org/10.1208/s12249-020-01909-4), PMID 33404984.
28. Rusdin A, Mohd Gazzali A, Ain Thomas N, Megantara S, Aulifa DL, Budiman A et al. Advancing drug delivery paradigms: polyvinyl pyrrolidone (PVP)-based amorphous solid dispersion for enhanced physicochemical properties and therapeutic efficacy. Polymers. 2024;16(2):286. doi: [10.3390/polym16020286](https://doi.org/10.3390/polym16020286), PMID 38276694.
29. Ha ES, Choo GH, Baek IH, Kim MS. Formulation, characterization, and *in vivo* evaluation of celecoxib-PVP solid dispersion nanoparticles using supercritical antisolvent process. Molecules. 2014;19(12):20325-39. doi: [10.3390/molecules191220325](https://doi.org/10.3390/molecules191220325), PMID 25486246.
30. Kapourani A, Tzakri T, Valkanioti V, Kontogiannopoulos KN, Barmpalexis P. Drug crystal growth in ternary amorphous solid dispersions: effect of surfactants and polymeric matrix-carriers. Int J Pharm X. 2021;3:100086. doi: [10.1016/j.ijpx.2021.100086](https://doi.org/10.1016/j.ijpx.2021.100086). PMID 34151251.
31. Knopp MM, Nguyen JH, Becker C, Francke NM, Jørgensen EB, Holm P, et al. Influence of polymer molecular weight on *in vitro* dissolution behavior and *in vivo* performance of celecoxib:PVP amorphous solid dispersions. Eur J Pharm Biopharm. 2016;101:145-51. doi: [10.1016/j.ejpb.2016.02.007](https://doi.org/10.1016/j.ejpb.2016.02.007). PMID 26899127.
32. Dontireddy R, Crean AM. A comparative study of spray-dried and freeze-dried hydrocortisone/polyvinyl pyrrolidone solid dispersions. Drug Dev Ind Pharm. 2011;37(10):1141-9. doi: [10.3109/03639045.2011.562213](https://doi.org/10.3109/03639045.2011.562213), PMID 21615280.
33. Kunz C, Gieseler H. Factors influencing the retention of organic solvents in products freeze-dried from co-solvent systems. J Pharm Sci. 2018;107(8):2005-12. doi: [10.1016/j.xphs.2018.04.001](https://doi.org/10.1016/j.xphs.2018.04.001). PMID 29649470.
34. Tchessalov S, Maglio V, Kazarin P, Alexeenko A, Bhatnagar B, Sahni E, et al. Practical advice on scientific design of freeze-drying process: 2023 update. Pharm Res. 2023;40(10):2433-55. doi: [10.1007/s11095-023-03607-9](https://doi.org/10.1007/s11095-023-03607-9), PMID 37783925.
35. Kittaka S, Kuranishi M, Ishimaru S, Umahara O. Phase separation of acetonitrile-water mixtures and minimizing of ice crystallites from there in confinement of MCM-41. J Chem Phys. 2007;126(9):091103. doi: [10.1063/1.2712432](https://doi.org/10.1063/1.2712432), PMID 17362095.
36. Vessot S, Andrieu J. A Review on Freeze Drying of Drugs with tert -Butanol (TBA) + Water Systems: characteristics, Advantages, Drawbacks. Drying Technol. 2012;30(4):377-85. doi: [10.1080/07373937.2011.628133](https://doi.org/10.1080/07373937.2011.628133).
37. Cerar J, Jamnik A, Pethes I, Temleitner L, Pusztai L, Tomšič M. Structural, rheological and dynamic aspects of hydrogen-bonding molecular liquids: aqueous solutions of hydrotropic tert-butyl alcohol. J Colloid Interface Sci. 2020;560:730-42. doi: [10.1016/j.jcis.2019.10.094](https://doi.org/10.1016/j.jcis.2019.10.094). PMID 31704003.
38. Bhatnagar BS, Sonje J, Shalaev E, Martin SW, Teagarden DL, Suryanarayanan R. A refined phase diagram of the tert-butanol-water system and implications on lyophilization process optimization of pharmaceuticals. Phys Chem Chem Phys. 2020;22(3):1583-90. doi: [10.1039/C9CP06576H](https://doi.org/10.1039/C9CP06576H), PMID 31894786.
39. International Council for Harmonisation (ICH). In: <https://www.ich.org>. Vol. R2: validation of analytical procedures. Geneva: ICH; 2022. Available. ICH guideline Q2 [cited 2026 Jan 10].
40. Cherif A, Deshmukh J, Sanil K, Taha I, Treffer D, Ashour EA. Towards enhanced solubility of cannabidiol: preparation and evaluation of cannabidiol solid dispersions using vacuum compression molding. AAPS PharmSciTech. 2025;26(3):83. doi: [10.1208/s12249-025-03078-8](https://doi.org/10.1208/s12249-025-03078-8), PMID 40069513.
41. Andriotis EG, Chachlioutaki K, Monou PK, Bouropoulos N, Tzetzis D, Barmpalexis P, et al. Development of water-soluble electrospun fibers for the oral delivery of cannabinoids. AAPS PharmSciTech. 2021;22(1):23. doi: [10.1208/s12249-020-01895-7](https://doi.org/10.1208/s12249-020-01895-7), PMID 33400042.
42. Zhang Z, Tan S, Feng SS. Vitamin E TPGS as a molecular biomaterial for drug delivery. Biomaterials. 2012;33(19):4889-906. doi: [10.1016/j.biomaterials.2012.03.046](https://doi.org/10.1016/j.biomaterials.2012.03.046), PMID 22498300.
43. Kabanov AV, Batrakova EV, Alakhov VY. Pluronic block copolymers as novel polymer therapeutics for drug and gene delivery. J Control Release. 2002;82(2-3):189-212. doi: [10.1016/S0168-3659\(02\)00009-3](https://doi.org/10.1016/S0168-3659(02)00009-3), PMID 12175737.
44. Pironi AM, Eloy JdO, Rodero CF, Antonio SG, Alonso JD, Chorilli M. PVP solid dispersions containing poloxamer 407 or TPGS for the improvement of ursolic acid release. Braz J Pharm Sci. 2023;59:e21217. doi: [10.1590/s2175-97902023e21217](https://doi.org/10.1590/s2175-97902023e21217).
45. Ha JM, Kang SY, Park CW, Bin SA, Rhee YS, Seo JW, et al. Effect of poloxamer on physicochemical properties of tacrolimus solid dispersion improving water solubility and dissolution rate. J Pharm Investig. 2012;42(4):171-6. doi: [10.1007/s40005-012-0025-4](https://doi.org/10.1007/s40005-012-0025-4).
46. Taylor LS, Zografi G. Spectroscopic characterization of interactions between PVP and indomethacin in amorphous molecular dispersions. Pharm Res. 1997;14(12):1691-8. doi: [10.1023/A:1012167410376](https://doi.org/10.1023/A:1012167410376). PMID 9453055.
47. Ugur BE, Caggiano NJ, Monson S, Bechtold AG, Seo Y, Prud'homme RK, et al. Molecular interactions underlying dissolution trends in cannabidiol-polymer amorphous solid dispersions. Macromolecules. 2024;57(17):8287-97. doi: [10.1021/acs.macromol.4c01579](https://doi.org/10.1021/acs.macromol.4c01579).
48. Ministry of Public Health (Thailand). Notification of the Ministry of Public Health. B.E. 2021;2564(428) issued under the Food Act B.E. 2522: food products containing cannabis extract as an ingredient. Royal Thai Government Gazette. 2021;138(Special Issue 198 Ng):9.